

show the time variant location of the solid-liquid interface and the surface temperature history. The heat capacity for this case is in terms of $pc = 1 + 0.01 T$ and b_1 is a parameter. The solid lines represent the results for which the heat flux is an exponential function of time, and the dash lines correspond to the situation with the heat flux being a linear function of time. The results with constant thermal properties are also included for the purpose of comparison. The same type of curves are presented in Figs. 3-4 with b_1 fixed and b_2 varied. It is seen that the quantity b_1 tends to increase s and decrease T_0 but the increase of b_2 reduces both s and T_0 . Furthermore, the variation of b_2 does not affect the melting rate very much, although it influences the surface temperature considerably.

References

- Imber, M. and Huang, P.N.S., "Phase Change in a Semi-Infinite Solid with Temperature Dependent Thermal Properties," *International Journal Heat and Mass Transfer*, Vol. 16, No. 10, Oct. 1973, pp. 1951-1954.
- Goodman, T.R., "The Heat Balance Integral and Its Application to Problems Involving a Change of Phase," *Transactions of the ASME*, Vol. 80, No. 3, Feb. 1958, pp. 335-342.
- Westphal, K.O., "Series Solution of Freezing Problem With The Fixed Surface Radiation Into A Medium of Arbitrary Varying Temperature," *International Journal Heat and Mass Transfer*, Vol. 10, No. 2, Feb. 1967, pp. 195-205.
- Prasad, A. and Agrawal, H.C., "Biot's Variable Principle For Aerodynamic Ablation of Melting Solids," *AIAA Journal*, Vol. 12, 1974, pp. 250-252.

Stability of Laser Heated Flows

P. K. S. Wu* and A. N. Pirri*
Physical Sciences Inc., Wakefield, Mass.

Introduction

THE success of any system designed to convert high power laser radiation into directed kinetic energy depends upon the ability of the system to perform this conversion efficiently. Neither the work on laser propulsion^{1,3} nor Hertzberg et al.⁴ have *a priori* addressed the fundamental issue of the most efficient process by which a flowing gas can absorb laser radiation and convert it to useful work. Pirri et al.^{1,2} relied upon the creation of electrons via breakdown to initiate absorption by inverse Bremsstrahlung and subsequent conversion of the heated gas into kinetic energy to obtain high specific impulse. However, these experiments illustrated *a posteriori* that without some tailoring of the propellant composition, the conversion process yields the initiation of absorption waves in the gas.² This results in unsteady flow behavior and low power conversion efficiency.

The stability of radiatively heated flows along with suggestions for acoustic wave amplification by radiative absorption have been examined to some extent by many authors.⁵ However, due to the inhomogeneity in the one-dimensional nozzle flow, when the disturbances are introduced, the full eigenvalue problem is rather difficult. Fortunately, much can be learned about wave propagation without solving the full boundary value problem, and information can be extracted from a study of the modified dispersion relation. To obtain the modified dispersion relation in inhomogeneous media the actual disturbance is ap-

proximated by harmonic functions over a small distance (small compared with the characteristic lengths associated with the gradients of the flow), and, hence, the analysis is only an accurate description "locally." The procedure is commonly used in problems of this type, e.g., Monsler⁶ has examined the instability of radiative transfer between two infinite plates. Here we apply the "local" stability analysis to a given nozzle to obtain contour (or contours) of neutral stability.

Method of Analysis

For simplicity, consider a one-dimensional flow through a nozzle of variable area ratio that is heated by laser radiation. The laser beam enters from the up-stream direction. The governing equations for the quasi-one-dimensional flow without viscous dissipation, diffusion, and thermal conduction but including radiative heat transfer are

$$\frac{\partial}{\partial t} (\rho A) + \frac{\partial}{\partial x} (\rho u A) = 0 \quad (1)$$

$$\frac{\partial u}{\partial t} + u \frac{\partial u}{\partial x} + \frac{1}{\rho} \frac{\partial p}{\partial x} = 0 \quad (2)$$

$$\frac{\partial h_s}{\partial t} + u \frac{\partial h_s}{\partial x} - \frac{1}{\rho} \frac{\partial p}{\partial t} = \frac{1}{\rho A} \frac{d(IA)}{dx} \quad (3)$$

where ρ is the density; u is the velocity; A is the area; p is the pressure; h_s is the stagnation enthalpy; and I is the intensity. For the radiative source term, it is assumed that

$$IA = I_0 A_i e^{-\tau}$$

where τ is the optical depth defined as⁷

$$\tau = \int_0^x \kappa dx \quad (4)$$

and a generalized absorption coefficient κ is assumed to be of the form

$$\kappa = \kappa_c \rho^n T^m \quad (5)$$

where κ_c is a constant; T is the gas temperature; and n and m are constants characterizing the absorber. All radiation quantities (I , I_0 , κ , τ , κ_c) are quasi-monochromatic in the sense of Ref. 8. Finally the equation-of-state, $p = \rho R T$, together with Eqs. (1-3) provide the necessary equations for variables ρ , u , p , and T .

The governing equations for the steady-state solutions are the same as the previous equations with the time derivatives set equal to zero. Substituting Eq. (4) into Eq. (3) and integrating the resulting steady-state energy equation yields

$$h_s(\tau) = I + \Gamma(1 - e^{-\tau})$$

where the stagnation enthalpy is normalized by its initial value h_{si} and the important parameter Γ , the ratio of laser power to the initial total energy flux of the flow, is defined as

$$\Gamma = (IP / (\rho u A h_{si}))$$

where IP is the laser power.

A general method of solution for the steady-state equations may be employed.⁹ The governing equations can be combined to yield a relationship which governs the Mach number variation through the nozzle.

$$\frac{dM^2}{d\tau} = \frac{1}{1-M^2} \left[1 + \frac{(\gamma-1)}{2} M^2 \right] M^2 \left[(1+\gamma M^2) \times \frac{1}{h_s} \frac{dh_s}{d\tau} - \frac{2}{A} \frac{dA}{d\tau} \right] \quad (6)$$

Received August 7, 1975; revision received December 3, 1975. This work was sponsored by NASA-Lewis, under Contract NAS3-18528 and NASA Project Manager, Mr. Stephen M. Cohen.

Index category: Hydrodynamics; Nozzle and Channel Flow; Electric and Advanced Space Propulsion.

*Principal Scientist. Member AIAA.

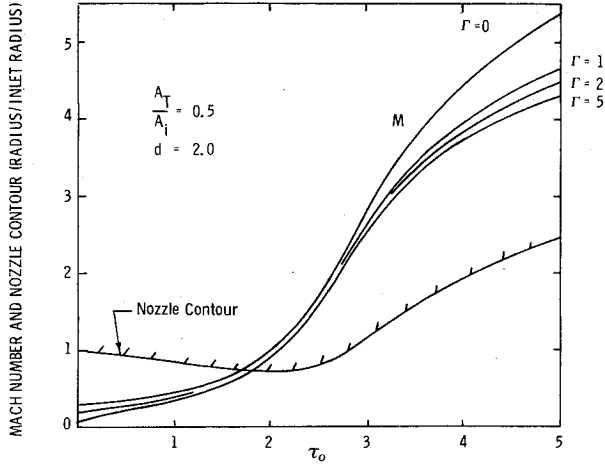


Fig. 1 Mach number distribution along the nozzle.

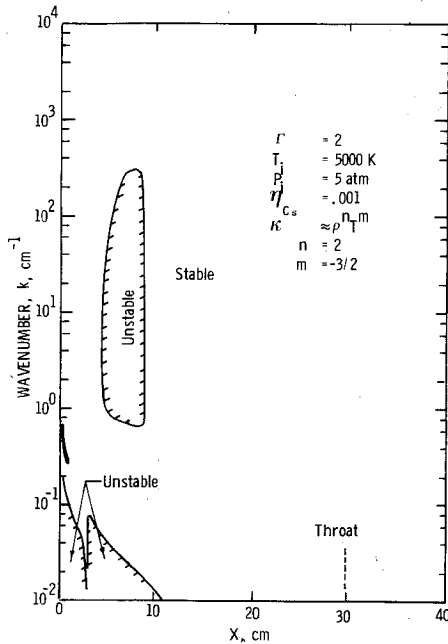


Fig. 2 Curves of neutral stability for $\Gamma = 3$ in physical dimensions.

where M is the Mach number. For convenience, the nozzle contour consists of two parts; up to $\tau = 3$ the one parameter nozzle configuration of Buonadonna et al.,⁸

$$\frac{A}{A_i} = 1 + \left[\frac{A_T}{A_i} - 1 \right] \frac{(1+d-\tau)e^\tau - (1+d)}{e^d - (1+d)}$$

where A_i is the initial area ($\tau = 0$), and A_T is the throat area located at $\tau = d$, and a parabolic section ($3 \leq \tau < 5$) as shown in Fig. 1. Equation (6) can now be integrated to yield the Mach

number distribution. Knowing the Mach number profile, the inlet conditions, and the laser power, one can proceed to calculate the complete steady-state solution, i.e., ρ , u , p , and T .

Stability Analysis

Due to the complexity in solving the full eigenvalue problem, a local stability analysis is utilized to determine the stability of disturbances generated at each point along the nozzle.

Combining Eqs. (4) and (5), one has

$$(\partial \tau / \partial x) = \kappa_c \rho^n T^m \quad (7)$$

Hence the governing equations for the stability analysis are Eqs. (1-3) and (7) for ρ , u , T , and τ . The pressure is eliminated by means of the equation-of-state. Now we can proceed to perturb the previously obtained steady flowfield by assuming

$$\rho = \rho_o(x) + \rho'(x, t)$$

where ρ_o is the known steady-state solution, and the prime indicates the small perturbations, i.e., $\rho' \ll \rho_o$. Neglecting the second or higher order terms yields a linear set of equations for the perturbation quantities. The coefficients in the perturbation equations are only functions of the steady-state variables and hence, for the sake of simplicity, the previous equations are nondimensionalized with respect to the steady-state variables, i.e.,

$$\bar{\rho} = \frac{\rho'}{\rho_o}; \bar{u} = \frac{u'}{u_o}; \bar{x} = \frac{x}{L} \text{ and } \bar{t} = \frac{tu_o}{L}$$

where the characteristic length L is taken to be $1/\kappa_o$ and κ_o is the steady-state absorption coefficient. Finally, the steady-state flowfield is assumed to be perturbed at a given location by a disturbance which is composed of a number of discrete partial fluctuations (harmonics). The perturbations representing a single oscillation of the disturbance are assumed to be of the form

$$\bar{\rho} = \hat{\rho}(\Omega, K) e^{i(K\bar{x} - \Omega\bar{t})} \quad (8)$$

where $\hat{\rho}$ is the amplitude function for $\bar{\rho}$. Similar assumptions are made for \bar{u} , \bar{T} , and $\bar{\tau}$. The nondimensional wavenumber K is a real quantity and $\lambda = 2\pi L/K$ is the wavelength of the disturbance. The quantity, $\Omega = \Omega_r + i\Omega_i$, where $\Omega_r u_o/L$ (amplification factor) determines the degree of amplification or damping. The disturbance is damped if $\Omega_i < 0$ and the steady-state flowfield is stable, whereas for $\Omega_i > 0$ instability sets in. The velocity of propagation of the wave in the x -direction (phase velocity) is given by

$$C = (\Omega_r/K) u_o$$

Substituting Eq. (8) into the nondimensional perturbation equations one gets a homogeneous set of equations for $\hat{\rho}$, \hat{u} , \hat{T} , and $\hat{\tau}$. In order that the solutions exist, the determinant of the coefficient matrix must vanish. Hence, we have

$$\begin{bmatrix} \frac{\partial}{\partial \bar{x}} \hat{m} u_o + \frac{\partial}{\partial \bar{x}} \hat{m} A - i\Omega + iK & \frac{\partial}{\partial \bar{x}} \hat{m} \rho_o + \frac{\partial}{\partial \bar{x}} \hat{m} A + iK & 0 & 0 \\ \frac{\partial}{\partial \bar{x}} \hat{m} u_o + \alpha \frac{\partial}{\partial \bar{x}} \hat{m} T_o + i\alpha K & \frac{\partial}{\partial \bar{x}} \hat{m} u_o - i\Omega + iK & \alpha \frac{\partial}{\partial \bar{x}} \hat{m} \rho_o + i\alpha K & 0 \\ \frac{\gamma}{\gamma-1} \alpha \frac{\partial}{\partial \bar{x}} \hat{m} T_o - \Gamma' n & \frac{\gamma}{\gamma-1} \alpha \frac{\partial}{\partial \bar{x}} \hat{m} T_o + iK & i \frac{\gamma \alpha}{\gamma-1} K - \Gamma' m' & \Gamma' \\ + \frac{\partial}{\partial \bar{x}} \hat{m} u_o + i\alpha \Omega & + 2 \frac{\partial}{\partial \bar{x}} \hat{m} u_o - i\alpha \Omega & - \frac{i\alpha}{\gamma-1} \Omega & \\ -n & 0 & -m & iK \end{bmatrix} = 0$$

where γ is the ratio of specific heats; $\alpha = RT_o/u_o^2$; and $\Gamma' = \Gamma h_{so} e^{-\tau_o/u_o^2}$. This is the modified dispersion relation and provides the relationship between the real K and the complex Ω . The method of solution is to assume K and, then, solve for the complex Ω (3 roots) for each location along the nozzle. This corresponds to applying an infinitesimal disturbance of wavelength $2\pi L/K$ at each location and to examine whether the disturbance will grow ($\Omega_i > 0$) or decay ($\Omega_i < 0$). The locus of $\Omega_i = 0$ defines a line (or lines) of neutral stability.

Results and Discussion

Solutions have been obtained for various nozzle configurations. However, for conciseness, we only present one set of example calculations, namely $d=2$ and $A_T/A_i=0.5$. As shown in Fig. 1, the Mach number distributions for this particular nozzle configuration are plotted as functions of τ_o , the optical depth in the steady-state flowfield. Hence the other flow properties such as ρ , u , and T can be calculated. For a given absorber, one can readily transform these results into the physical space by inverting Eq. (4).

The stability map for $\Gamma=2$ is presented in Fig. 2. These results are for an absorption coefficient of the form, $\kappa \sim \rho^2 T^{-3/2}$, which corresponds to inverse Bremsstrahlung absorption via electrons. The initial temperature T_i and pressure p_i are assumed to be 5000 K and 5 atm, respectively. The glowing gas is taken to be helium with seeded cesium (mole fraction of .001) and the cesium is assumed to be completely ionized to provide sufficient electrons for absorption by inverse Bremsstrahlung.

As shown in Fig. 2, the wavenumber k is plotted against the axial distance with contours of $\Omega_i = 0$. These contours form the boundary between stable and unstable regions in wavenumber space. At each nozzle location, the shaded zone indicates the range of wavenumbers which results in growing disturbances. The unstable zones are located from $x=0$ to $x=10$ cm in the region where the absorption takes place. Therefore, if a disturbance has a wavelength much greater than 10 cm, the absorption will only affect a fraction of the wave, and growth of the entire wave will not be significant. Since $k = 2\pi/\lambda$ where λ is the disturbance wavelength, this implies that only $k \lesssim 6 \text{ cm}^{-1}$ are of interest. Hence, the uppermost unstable zone is the only physically important region. It is now desirable to make this region as small as possible to minimize the possibility of unstable heating in the nozzle. It must be remembered that this analysis will not tell us whether a disturbance, which is initiated and grows in one region, will dampen after it travels to a new location. Nevertheless the analysis serves as an important indicator as to where potential absorption wave phenomena may be initiated.

References

- ¹Pirri, A. N. and Weiss, R. F., "Laser Propulsion," AIAA Paper 72-719, Boston, Mass., 1972.
- ²Pirri, A. N., Monsler, M. J., and Nebolsine, P. E., "Propulsion by Absorption of Laser Radiation, AIAA Paper 73-624, Palm Springs, Calif., 1973.
- ³Rom, F. E. and Putre, H. A., "Laser Propulsion," NASA TM-X-2510, April 1972.
- ⁴Hertzberg, A., Johnston, E. W., and Ahlstrom, H. G., "Photon Generators and Engines for Laser Power Transmission," AIAA Paper 71-106, New York, New York, 1971.
- ⁵Vincenti, W. G. and Traugott, S. C., "The Coupling of Radiative Transfer and Gas Motion," *Annual Review of Fluid Mechanics*, Vol. 3, 1971, pp. 89-117.
- ⁶Monsler, M. J., "An Acoustic Instability Driven by Absorption of Radiation in Gases," PhD thesis, M.I.T., Dept. of Aeronautics and Astronautics, Cambridge, Mass., 1969.
- ⁷Vincenti, W. G. and Kruger, C. H., Jr., *Introduction to Physical Gas Dynamics*, Wiley, New York, 1965, p. 463.
- ⁸Buonadonna, V. R., Knight, C. R., and Hertzberg, A., "The Laser Heated Wind Tunnel," *AIAA Journal*, Vol. 11, Nov. 1973, pp. 1457-1458.
- ⁹Shapiro, A. H., *Compressible Fluid Flow*, The Ronald Press Co., New York, Vol. 1, 1953.

On Optimum Design of Prestressed Beam Structures

Lewis P. Felton*

University of California, Los Angeles, Calif.

Introduction

A COMPREHENSIVE nonlinear programming formulation of the optimization problem for multiply loaded indeterminate structures, containing design variables associated with diverse forms of prestressing, previously has been presented.¹ Several optimized trusses were examined, and it was shown, e.g., that prestress resulting from lack of fit (i.e., initial element deformations) provided significant reductions in truss weight and led to an otherwise nonfully stressed truss being fully stressed.

It is the purpose of this Note to demonstrate the possible advantages of similar prestressing in beam-type structures. In particular, prestressing by initial deformations will be illustrated for a class of thin-walled indeterminate structures which has been investigated in recent optimization studies.^{2,3} This class of structures is well suited to the present application for several reasons. First, optimized thin-walled structures, which satisfy local buckling criteria, provide rational lower bounds on weight. Second, the design problem has been reduced to a particularly simple form, involving only moments of inertia of the elements and prestressing parameters as design variables, and is devoid of inequality behavioral and side constraints, with the exception of non-negativity requirements for moments of inertia and, possibly, limits on the prestressing variables. Finally, optimized unstressed structures of this class are inherently fully stressed, although maximum stresses vary from element to element, and the effect of prestress on such structures thus should be of distinct interest.

Analysis of Beam Structures with Initial Deformations

Figure 1a shows a uniform beam element with initial deformations equivalent to a relative slope and displacement between ends, denoted, respectively, by θ_0 and δ_0 . The equilibrium equation for such an element may be given as

$$P = K\Delta + P_0 \quad (1)$$

where P is a vector of generalized element end forces of the types shown in Fig. 1b, Δ is a vector of associated generalized end displacements, K is the element stiffness matrix, and P_0 is interpreted as a vector of fixed-end forces due to applied loads or thermal or initial effects. For a beam with initial displacements as in Fig. 1a, it may be shown that the fixed-end moments M_{10} and M_{20} are given, respectively, by

$$M_{10} = (2EI/\ell) [\theta_0 - (3\delta_0/\ell)] \quad (2a)$$

$$M_{20} = (2EI/\ell) [2\theta_0 - (3\delta_0/\ell)] \quad (2b)$$

where E is Young's modulus and I is moment of inertia. Fixed-end shears V_{10} and V_{20} follow directly from element equilibrium.

The equilibrium equation for an assemblage of these elements is given by

$$F = ku + \beta^T \bar{P}_0 \quad (3)$$

Received Nov. 12, 1975. This research was supported by AFOSR Grant No. 74-2640A, W. Walker, Program Manager, L. A. Schmit Jr., R. B. Nelson, and L. P. Felton, co-principal investigators.

Index category: Structural Design, Optimal.

*Associate Professor, Mechanics and Structures Department. Associate Fellow AIAA.